



## Engineering design and prototype development of a full scale ultrasound system for virgin olive oil by means of numerical and experimental analysis



Maria Lisa Clodoveo<sup>a,\*</sup>, Vito Moramarco<sup>b</sup>, Antonello Paduano<sup>a</sup>, Raffaele Sacchi<sup>c</sup>, Tiziana Di Palma<sup>a</sup>, Pasquale Crupi<sup>a</sup>, Filomena Corbo<sup>d</sup>, Vito Pesce<sup>e</sup>, Elia Distaso<sup>b</sup>, Paolo Tamburrano<sup>b</sup>, Riccardo Amirante<sup>b</sup>

<sup>a</sup> Department of Agricultural and Environmental Science, University of Bari, Via Amendola 165/A, 70126 Bari, Italy

<sup>b</sup> Department of Mechanics, Mathematics and Management (DMMM), Polytechnic University of Bari, Via Orabona 4, Italy

<sup>c</sup> Department of Agriculture, University of Naples Federico II, Via Università 100, 80055 Portici, NA, Italy

<sup>d</sup> Department of Pharmaceutical Chemistry, University of Bari, Bari, Via Orabona, 4, Italy

<sup>e</sup> Department of Biosciences, Biotechnologies and Biopharmaceutics, University of Bari, Via Orabona, 4, 70126 Bari, Italy

### ARTICLE INFO

#### Article history:

Received 17 May 2016

Received in revised form 1 November 2016

Accepted 5 January 2017

Available online 6 January 2017

#### Keywords:

Virgin olive oil process

Ultrasound

Fluid dynamic analysis

Virgin olive oil quality

### ABSTRACT

The aim of the virgin olive oil extraction process is mainly to obtain the best quality oil from fruits, by only applying mechanical actions while guaranteeing the highest overall efficiency. Currently, the mechanical methods used to extract virgin oils from olives are basically of two types: the discontinuous system (obsolete) and the continuous one. Anyway, the system defined as “continuous” is composed of several steps which are not all completely continuous, due to the presence of the malaxer, a device that works in batch. The aim of the paper was to design, realize and test the first full scale sono-exchanger for the virgin olive oil industry, to be placed immediately after the crusher and before the malaxer. The innovative device is mainly composed of a triple concentric pipe heat exchanger combined with three ultrasound probes. This mechanical solution allows both the cell walls (which release the oil droplets) along with the minor compounds to be destroyed more effectively and the heat exchange between the olive paste and the process water to be accelerated. This strategy represents the first step towards the transformation of the malaxing step from a batch operation into a real continuous process, thus improving the working capacity of the industrial plants. Considering the heterogeneity of the olive paste, which is composed of different tissues, the design of the sono-exchanger required a thorough fluid dynamic analysis. The thermal effects of the sono-exchanger were monitored by measuring the temperature of the product at the inlet and the outlet of the device; in addition, the measurement of the pigments concentration in the product allowed monitoring the mechanical effects of the sono-exchanger. The effects of the innovative process were also evaluated in terms of extra virgin olive oil yields and quality, evaluating the main legal parameters, the polyphenol and tocopherol content. Moreover, the activity of the polyphenol oxidase enzyme in the olive paste was measured.

© 2017 Elsevier B.V. All rights reserved.

### 1. Introduction

Olive trees are an economic and social resource in the Mediterranean basin [1]. Virgin olive oil (VOO) is the main component of the Mediterranean diet due to its excellent sensory and nutritional qualities, and the benefits of consuming olive oil have been known since antiquity [2]. This because olive fruit contains a good concentration of hydrophilic (phenolic acids, phenolic alcohols, flavonoids, and secoiridoids) and lipophilic phenolic compounds which are known to possess multiple biological properties such

as antioxidant, anticarcinogenic, antimicrobial, antihypertensive, cardioprotective and antiplatelet benefits [3]. Manufacturers and researchers are currently focused on better understanding the key elements that allow modulating the complex series of physical, physico-chemical, chemical and biochemical transformations occurring during the EVOO elaboration, in order to develop innovative and sustainable plant solutions able to increase both the yield and the quality of products [4–6]. Currently, the mechanical methods used to extract virgin oils from olives are basically of two types: the discontinuous system (obsolete) and the continuous one. The discontinuous-type system is dying out because it is characterized by a very low work capacity [7] requiring great workforce. The “continuous-type” is generally made up of a

\* Corresponding author.

E-mail address: [marialisa.clodoveo@uniba.it](mailto:marialisa.clodoveo@uniba.it) (M.L. Clodoveo).

mechanical crusher, a few malaxers required to ensure continuity to the process, and a centrifugal decanter to separate the oily phase. The “continuous” appellation refers to the fact that the mechanical crusher, decanter and vertical-axis centrifugal separator operate continuously; in contrast, the malaxer, which is actually a machine working in batches, is located between these two continuous apparatuses. For this reason the malaxation represents the bottleneck of the continuous extraction process [6]. Moreover, the malaxer is a heat-exchanger characterized by a large volume combined with a small surface, which makes the heat exchange highly inefficient. The industrial challenge of the VOO plant manufacturing sector is to design and produce advanced machines in order to transform the discontinuous malaxing step into a fully continuous phase, thus improving the working capacity of the industrial plants as well as the efficiency of the heat exchange [8,9].

Ultrasound (US) is a promising emerging technology that has already found application in the food industry [10–12] due to its significant effects on the processes, such as higher product yields, shorter processing times, reduced operating and maintenance costs, simplified manipulation and work-up, improved taste, texture, flavour and colour [13]. US has promising application also in the field of virgin olive oil industry, due to the mechanical and thermal effects useful to guarantee adequate oil yields, thus reducing the process time and improving the process efficiency [14–16]. Recently, Clodoveo and co-authors studied the mechanical and thermal effects of US on the virgin olive oil elaboration process by means of a pilot scale plant [17–20] and underlined that the US mechanical effects are due to the cavitation phenomena. When highly energetic ultrasonic waves are conveyed into liquids, the alternating high pressure and low pressure cycles create bubbles or voids in the liquid. Those bubbles grow over several cycles until they cannot absorb more energy so that they collapse violently during a high pressure cycle. This phenomenon of violent bubble implosions, known as cavitation, is characterized by extreme local conditions, such as very high temperatures, high cooling rates, high pressure differentials, shock waves and liquid jets. The effects of cavitation promote the rupture of the solids that are in the liquid medium, thereby increasing both the total solid surface in contact with the liquid phase and the mass transfer [21–25]. In the case of the olive paste, cavitation by means of ultrasounds promotes the rupture of the cell walls that remained unbroken after the crushing phase in the crusher machine, releasing faster the oil and other minor compounds. Moreover, US can facilitate the mechanisms of thermal conduction and thermal convection if it is combined with a warming system, such as a heat-exchanger, due to the turbulence increment in the matter [26,27]. This phenomenon can significantly reduce the duration of malaxation, representing a first step towards an effective continuous process. Working towards the development of an innovative US equipment for the extraction of VOOs, Clodoveo et al. suggested combining an ultrasound system with a double-pipe heat exchanger. The main idea was to realize a more efficient heat exchange before pumping the olive paste into the malaxers, resolving another weakness of the currently used systems: the low overall heat transfer coefficient due to the disadvantageous ratio ( $r$ ) ( $r = S/V$ ) of the small malaxer surface area ( $S$ ) to the large volume ( $V$ ) of the olive paste [5]. In fact, in this way, a cheaper and simpler malaxing machine can be realized, thus excluding the jacket needed to heat the olive paste, providing only a thermal insulation to the tank. Starting from these previous evidences and hypothesis, an US system was designed, realized and tested in an industrial-scale VOO extraction plant. This innovative equipment, called “sono-exchanger”, which was engineered, designed and prototyped to be industrially exploitable, was evaluated in terms of energy and time necessary to maintain acceptable

yields of oils. A 3D fluid dynamic analysis was performed to evaluate the behaviour of the olive paste flowing around the ultrasound devices inside the sono-exchanger. The flow parameters of the olive paste were predicted, and in particular the pressure drops, because the adjustment of the pressure level is a way to control cavitation [28,29]. The influence of each geometrical parameter was studied to setup an optimal design of the sono-exchanger, which was subsequently tested experimentally. After the industrial tests, the chemical and the sensory evaluations of the resulting VOOs were performed. Polyphenol oxidase (PPO) is one of the enzymes involved in the phenol content reduction in the VOOs during the extraction process. In fact, after the cell structure is destroyed, and the enzymes and substrate are mixed, PPO catalyses the hydroxylation of monophenols (monophenolase) and oxidation of o-diphenols to o-quinones (diphenolase). Ultrasounds cause enzymes inactivation by cell lysis due to the cavitation bubbles implosion which generates spots of extremely high pressure and temperature, changing enzyme structural configuration and modifying its catalytic activity [30]. In order to verify this hypothesis, the activity of the PPO in the olive paste was measured with and without performing the ultrasound treatment.

## 2. Materials and methods

### 2.1. The industrial processing plant before and after the prototype installation

Fig. 1 shows the flow chart of a typical process, as it is available for the experimentation in the “Aloia” virgin olive oil extraction plant (Colletorto (CB), Italy). It consists in the usual, continuous-type process including the malaxing stage.

The plant consists of the following devices:

1. Fruits reception: here, the harvested olives are moved to the extraction plant. The olives are dropped into a hopper and laid down onto a conveyor belt that carries them to the washing machines.
2. Washing and leaf removal equipment: here, a vibrating screen and a blower remove leaves and other debris to protect the extraction plant and avoid the off-flavours deriving from the presence of foreign bodies. After that, the olives are also washed to remove soil or other residues. After the pre-process stage is finished, another conveyor belt carries the olives to the next phase.
3. Crushing equipment: this is the first phase of the extraction process. The aim of the crushing phase is the size reduction of olive fruit tissues and the breakdown of vegetal cells in order to facilitate the release of the oil by means of a strong mechanical action which also produces heat due to the energy dissipation. In this plant there is a hammer crusher, type Alfa Laval 25HP equipped with a 7 mm fixed grid and an electrical engine rotating at 2800 RPM. The olive paste obtained is moved to the following stage by means of a piping and an upstream mono pump.
4. Mono pump: it is a rotary positive displacement pump with an eccentric screw, also called progressive cavity pump (Bellin 600M2/K6, rotating at 125 RPM). This kind of pump is indicated for heavy-duty applications and can be used to pump abrasive pastes, viscous products, oils, sludge, emulsions etc. The pump is driven by an electrical engine controlled by means of a Toshiba Vf-Ps1 vector inverter, which regulates the rotational speed of the pump and so the olive paste flow rate.
5. Malaxer: It consists of a usual cylindrical tank equipped with a shaft with rotating arms and stainless steel blades. The walls of the malaxer are hollow allowing warm water to flow through

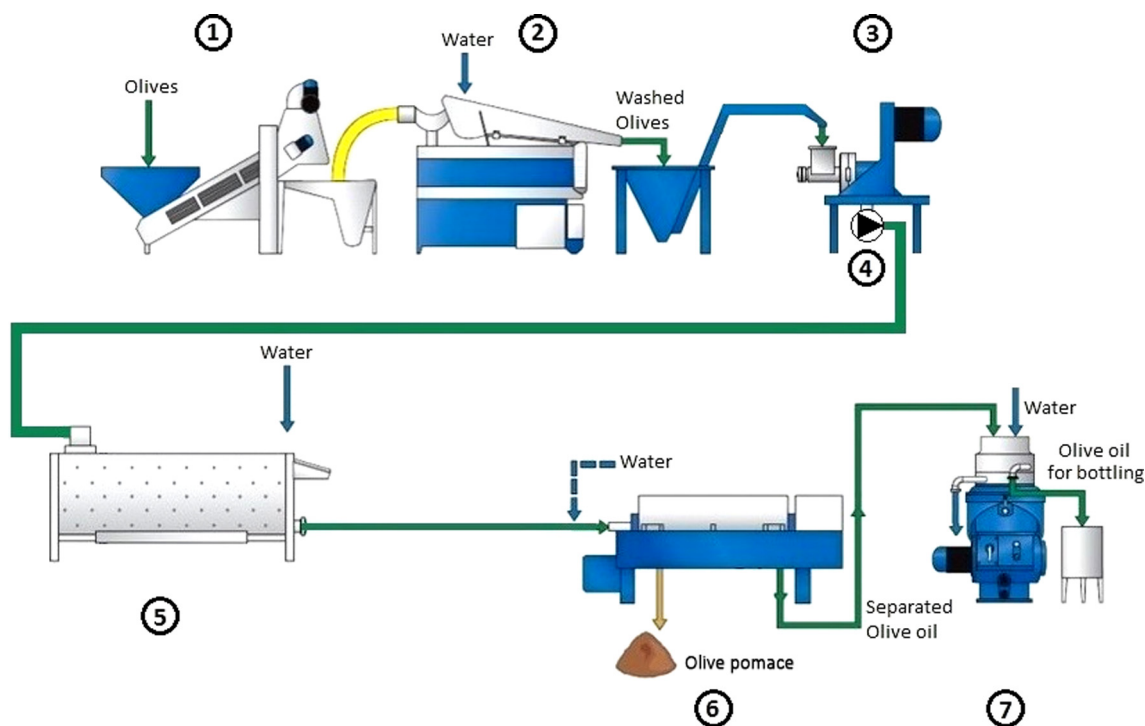


**Fig. 1.** Traditional continuous-type VOO extraction process scheme: 1, reception stage; 2, washing stage; 3, crushing stage; 4, mono pump; 5, malaxing stage; 6, separation stage; 7, clarification stage.

these jackets to heat the olive oil paste. During the malaxation phase the olive paste is continuously agitated at a controlled temperature. Heating process (25–30 °C) together with a low and continuous kneading phase of the olive paste (20–30 RPM for 30–45 min) are needed to help the small droplets of the oil formed during the milling to merge into large drops (coalescence phenomena), which can successively be separated easily through centrifugal systems. Due to very long process times and in order to reduce downtime, the manufacturing plant was provided with four simultaneously-working malaxers (Alfa Laval Atmosphere Module 650 – capacity of 650 L). In this way, it is possible to consider the process as almost continuous but at the expense of additional economic efforts [31]. Once the malaxing process has been completed, the paste is removed from the bottom of the tank by another pump which feeds the paste into a decanter centrifuge for the subsequent treatment.

6. **Decanter:** It is a horizontal centrifuge. In this equipment it is possible to perform the separation of the phases, namely the separation of oil from the solid and liquid phases of the olive paste. This installation uses Alfa Laval Uvnx-X20b-11g – stationary speed 3570 RPM, a three-phase centrifugal decanter where water is added to dilute the incoming paste, which is divided into extracted oil, vegetation water and solids (olive pomace).
7. **Vertical centrifuge:** (Alfa Laval Uvpx 507agt-14) it allows clarifying the extracted oily phase by adding lukewarm tap water. In this way, the equipment separates the residual water and the solid impurities in order to obtain clear oil.

This plant was modified by adding a “sono-exchanger” and a “heat-exchanger” downstream of the crusher and upstream of the malaxer, as shown in Fig. 2.

The sono-exchanger is made up of two straight pipes connected by an elbow, as shown in Fig. 3. A detailed fluid dynamic analysis is performed by means of Ansys Fluent in the following paragraphs to design the cross section of the device and the pipe curvature. Two

ultrasonic rod-style transducers (Sonopush Mono® 30–1500 W – 30 kHz) were plugged into the straight pipes through a bend. A third ultrasound transducer (30–1400 W output power) was placed downstream of the heat exchanger.

The ultrasonic probes inside the pipe determine the cavitation phenomenon within the olive paste along with a vibrational energy transferred to the olive paste. The heat exchanger is a ViscoLine™ annular heat exchanger (VLA) produced by Alfa Laval, suitable to non-Newtonian products with high viscosity and products that contain particulates. It can be used to perform a fast and fine tuning of the temperature of the olive paste before reaching the malaxer. The conditioning fluid is water flowing in opposite direction to the olive paste.

## 2.2. Engineering design and prototype development

### 2.2.1. The sono-exchanger and the fluid dynamic analysis

In many studies, experimental approaches have been applied; as an example, Legay et al. investigated the performances of a double-tube heat exchanger with and without the influence of ultrasonic vibrations [32]. However, preliminary experimental tests are usually expensive and time-consuming. For this reason, a 3D computational fluid dynamics (CFD) analysis was developed to gain insight into the flow inside the “sono-exchanger” and find the best position of the transducers that can provide the highest intensity of sonication. The problem of determining the pressure losses is important in order to achieve the indications needed to predict the cavitation phenomenon and to design the device and the pumping systems in a full-scale plant, thus avoiding expensive experimental tests. The pressure trend around the probes and so flow velocities are very important because the ultrasound energy exchange is strongly affected by the olive paste consistency. High discontinuities inside the flow, due to air bubbles, or separation flux phenomena worsen the ultrasound transmission. As a result, the need for and benefits of accurately predicting velocity profiles, concentration profiles and pressure drop of the flow during the

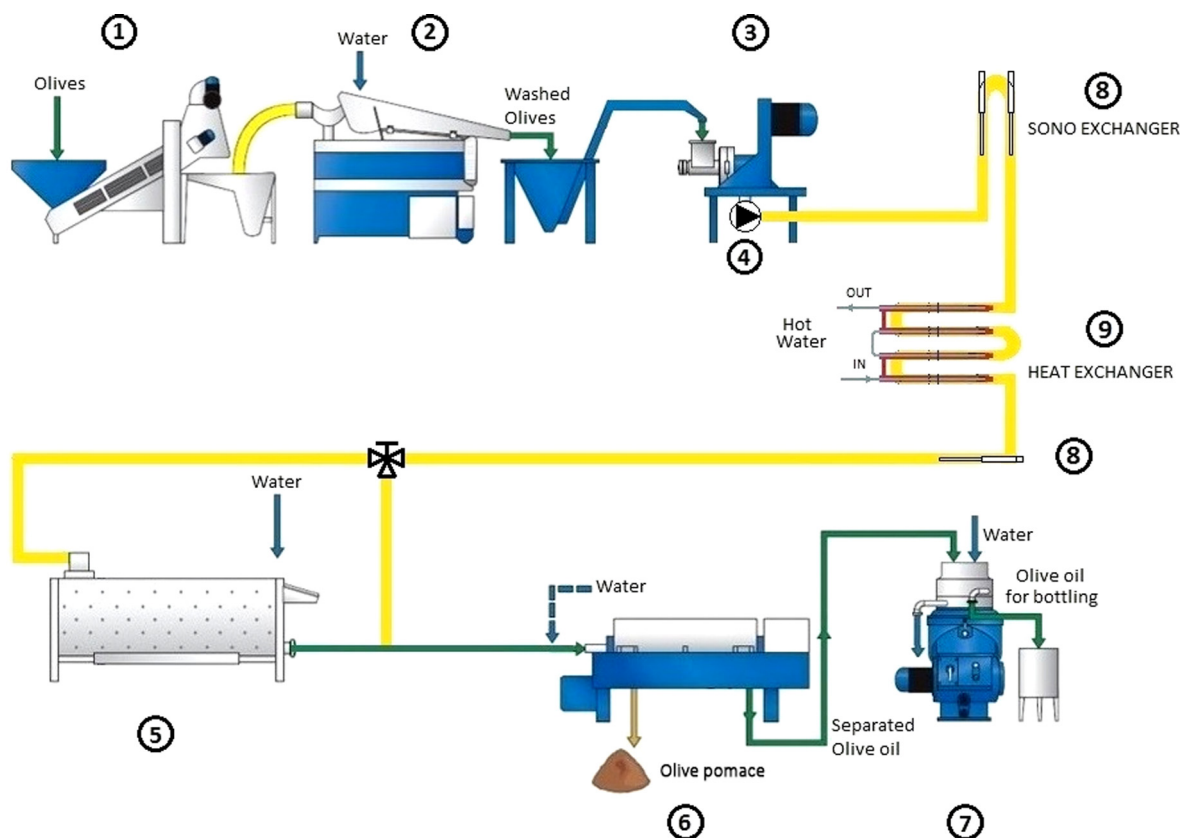


**Fig. 2.** VOO modified extraction process scheme: 1.reception stage; 2.washing stage; 3.crushing stage; 4.pump; 5.malaxing stage; 6.separation stage; 7.clarification stage; 8. Ultrasonic probes; 9.heat exchanger.



**Fig. 3.** Picture of the sono-exchanger system.

design phase is enormous and can also allow a better selection of the pumps, the optimization of power consumption, thereby helping maximize the economic benefit.

#### 2.2.2. Physical model

In the malaxation phase of the extraction process for virgin olive oil, the paste is usually highly viscous, thus showing a non-Newtonian behaviour (i.e. fluids that do not obey to Newton's law of viscosity and have an effective viscosity which is a function of the shear rate).

Therefore, it is important to understand the behaviour of non-Newtonian fluids to design the cross section of the device. The vis-

cosity of these fluids is highly dependent on their concentration or composition. In some cases, it is also affected by the history of the treatment such as cooling or heating, which can lead to large variations in the rheological behaviour. In particular, the rheological characteristics of the olive paste change from the inlet to the outlet of the olive extraction line [34]. Di Renzo and Colelli demonstrated that a non-Newtonian model, expressed by a power law relation, is capable of describing the rheological behaviour of the olive paste [35].

Experimental data on the apparent viscosity values and the related shear rates were collected; these data were processed by means of linear regression on a logarithmic scale to verify the

consistency of the power law model for the rheological behaviour of the olive paste.

### 2.2.3. Flow governing equations

The mass and momentum conservation equations for an incompressible fluid can be written as

$$\nabla \cdot v = 0 \quad (1)$$

$$\rho \left( \frac{\partial v}{\partial t} + v \cdot \nabla v \right) = -\nabla p + \nabla \cdot \tau \quad (2)$$

where  $\rho$  is the density,  $v$  is the velocity field,  $p$  is the pressure, and  $\tau$  is the deviatoric stress tensor related to the strain rate tensor.

Consider a fluid particle subjected to a shear stress  $\tau$  (Fig. 4); because this is deformed continuously under the action of a constant stress, the deformation speed must be determined.

Assuming that the upper surface of the particle is moving with a constant velocity  $v$ , in the time  $\Delta t$  it has covered the distance  $v\Delta t$ , thus producing the angular deformation:

$$\tan(\Delta\gamma) = \frac{v \cdot \Delta t}{y} \cong \Delta\gamma \quad (3)$$

The angular deformation speed, or shear rate, is given by:

$$\dot{\gamma} = \lim_{\Delta t \rightarrow 0} \frac{\Delta\gamma}{\Delta t} = \frac{\partial v}{\partial y} \quad (4)$$

And  $\frac{\partial v}{\partial y}$  is the gradient of velocity along the  $y$  dimension. It is possible to write the following relation:

$$\tau = \frac{\partial F}{\partial A} = \mu \frac{\partial v}{\partial y} = \mu \dot{\gamma} \quad (5)$$

where the shear rate  $\dot{\gamma}$  is proportional to the shear stress  $\tau$ , with the constant of proportionality being the viscosity  $\mu$ . For a Newtonian fluid  $\mu$  depends only on the nature of the fluid and its physical state, but the olive paste has a non-Newtonian behaviour (the viscosity decreases with the increasing velocity gradient). For non-Newtonian fluids, the stress-deformation rate equation can be written as:

$$\tau = \mu(\dot{\gamma})\dot{\gamma} \quad (6)$$

As mentioned above, to model the behaviour of this fluid, the power-law model can be used, whose equation is:

$$\tau = k\dot{\gamma}^n \quad (7)$$

The viscosity for the power-law model is obtained by dividing Eq. (7) by  $\dot{\gamma}$ :

$$\mu_{app} = k\dot{\gamma}^{n-1} \quad (8)$$

where  $\mu_{app}$  denotes an apparent or effective viscosity which is function of the shear rate,  $k$  is a measure of the average viscosity of the fluid (the consistency index), and  $n$  is a measure of the deviation of

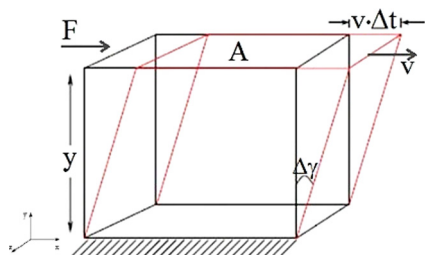


Fig. 4. Fluid deformation scheme.

the fluid from a Newtonian behaviour (the flow behaviour index, which is a dimensionless quantity). The value of  $n$  determines the class of the fluid:  $n = 1 \rightarrow$  Newtonian fluid  $n > 1 \rightarrow$  shear-thickening (dilatant fluids)  $n < 1 \rightarrow$  shear thinning (pseudo-plastics)

In the present setup, the dependency of  $k$  on the temperature is neglected.

### 2.2.4. Computational set-up

The finite-volume method was used to discretize and solve the coupled set of Eqs. (1) (7) (8) by employing the commercial software Ansys Fluent 15, using the pressure-based solver. In this approach, the pressure field is extracted by solving a pressure equation or pressure correction equation obtained by manipulating the continuity and momentum equations. The flow was modelled as laminar, due to the high viscosity of the olive paste, which remains laminar even at larger flow rates.

In Fluent the fluid (olive paste) was defined as incompressible, while the non-Newtonian power-law model was used for the viscosity. The properties of the fluids are shown in Table 1 for completeness. The heat transfer was neglected, the flow was considered steady, while the “simple” algorithm procedure was adopted to perform the coupling between the pressure and the velocity.

The interpolations for the velocities and pressures were based on a second-order discretization. The solutions were considered converged when both the normalized residuals were below  $1 \times 10^{-7}$  and the area weighted averages of the flow properties, evaluated on a cross section, reached stable values (with variations below 1% of the mean values). Overall, approximately 5000 iterations were necessary to respect this convergence criterion.

### 2.2.5. Grid generation

The numerical simulation process started with the creation of the geometry, while the second step was to mesh the geometry. In this study, an unstructured tetrahedral grid was used to comply with the curved structure of the geometry: triangular cells were used to mesh the surfaces of the tube walls, while the volume enclosed by these surfaces was meshed with parallelepiped and tetrahedral elements. The boundary conditions used for the inlet and outlet were defined as mass flow inlet and pressure outlet, respectively. In order to reduce the overall computational time, and taking advantage of the symmetry of the domain (see Fig. 5), only a half of the geometry was meshed.

A grid convergence analysis was carried out to reduce the total amount of CPU time, while maintaining a high solution accuracy. The effects of different grid sizes upon the flow solution were analysed; some of the grids used in the grid convergence study are reported in Fig. 6, which shows how the grid was refined starting from a baseline coarse mesh.

The grid shown in Fig. 6c was chosen, as it is the coarsest grids among those that provide high solution accuracy. The optimal grid was composed of 1.5 million elements with a skewness factor less than 0.825 (the worst element has a quality value of 0.8242). The mass flow rate and the outlet pressure were set equal to the experimental values, namely  $G_{inlet} = 0.278 \text{ kg/s}$  (equal to a half of the experimental value because only a half of the geometry was modelled) and  $p_{out} = 8 \text{ bar}$ .

Table 1  
Material properties and power-law parameters used.

Fluid	Density [kg/m <sup>3</sup> ]	Consistency Index, $k$ [Pa s <sup>n</sup> ]	Behaviour Index, $n$
Olive paste	1120	68	0.184

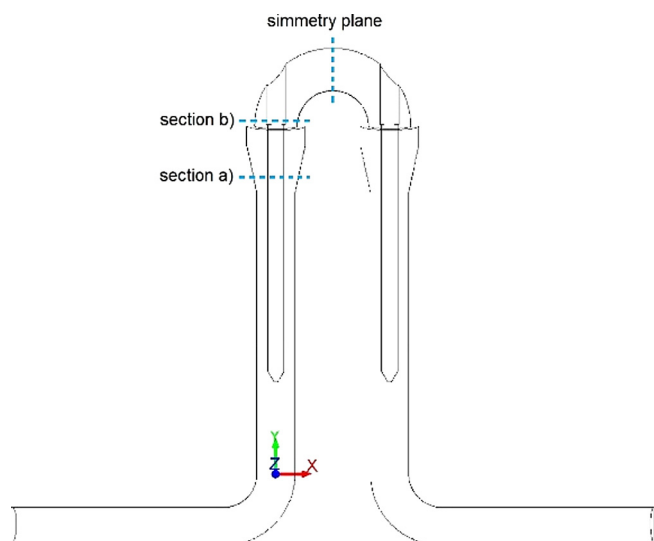


Fig. 5. a) Modelled sono-exchanger geometry; b) detail.

### 2.2.6. Energy transfer rate

The specific energy generated by the ultrasound transducers, to be conveyed to the olive paste in the pilot plant, must be set equal to the optimal value obtained from a preliminary analysis carried out in static conditions on small specimens using the same process experimented in previous studies. The optimal value of the specific energy,  $L_i$ , was obtained using the following equation:

$$L_i = \frac{P_s \cdot t}{m} \quad (9)$$

where  $P_s$  and  $t$  are the delivered power and the operating time of the transducer, respectively;  $m$  denotes the mass of the specimen.

Some analyses were conducted to assess the yield and quality of the oil obtained from various trials performed by changing the duration of the olive paste exposure to ultrasounds; in this way, the optimal exposure and energy transmitted were evaluated [12,33]. Having determined the optimal specific energy, it is possible to derive the optimal mass flow rate  $G_{id}$  that absorbs this energy while flowing inside the sono-exchanger, by using the following equation:

$$G_{id} = \frac{P_g}{L_i}$$

where  $P_g$  is the overall power emitted by the ultrasonic transducers and  $L_i$  is the optimal specific energy.

The size of the plant was chosen to obtain the optimal mass flow rate calculated in the static condition [12]. The actual mass flow rate provided by the volumetric pump (n. 4 in Fig. 2) is:

$$G_p = \rho \cdot V \cdot \tau \cdot n_{el} \cdot \eta_v$$

where  $\rho$  is the olive paste density,  $V$  the pump displacement,  $\tau$  the gear ratio of the transmission connecting the volumetric pump to the electric engine having a rotational speed equal to  $n_{el}$ , while  $\eta_v$  is the volumetric efficiency that depends both on the rotational speed and on the operating pressure.

To avoid discontinuity and air bubbles in the olive paste (see Fig. 7.a) delivered by the pump (see n. 4 of Fig. 2), because it is a high viscosity non-homogenous fluid, it is important to continuously adjust the mass flow processed by the crusher. To accomplish this task, it is possible to vary the conveyor belt velocity upstream of the crusher.

Because of this, during the normal operation conditions it is impossible to completely avoid the olive paste discontinuity; as a result, the actual power provided by the transducers must be reduced through an appropriate coefficient:

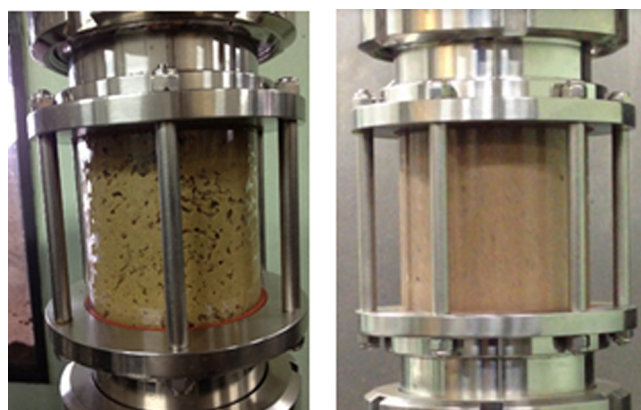


Fig. 7. Treated olive paste a) discontinuous; b) homogeneous.

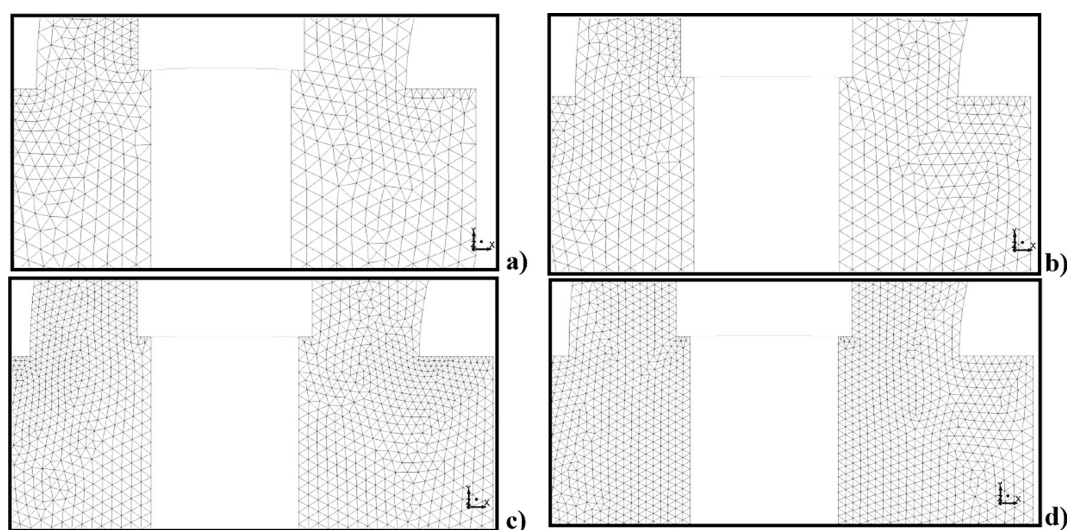


Fig. 6. Different grids used in the grid convergence study.

$$P = P_g \cdot \eta_d$$

where  $\eta_d$  is a dynamic exchange efficiency index that depends on the previous mentioned factors and allows calculating the actual power absorbed by the paste.

Typical values for  $\eta_d$  are around 0.75 when the paste is dense (Fig. 7.b); in contrast,  $\eta_d$  is lowered to 0.30–0.40 for very discontinuous olive pastes (Fig. 7.a).

### 2.3. Experimental campaign and quality indices

After having designed the sono-exchanger, a thorough experimental campaign was performed on the Aloia mill plant in harvesting season 2015. In the following sections the tests are described in detail, along with the quality indices that describe the performances of the proposed plant.

#### 2.3.1. Olives and oil samples

The experimental tests were performed in the Aloia mill plant fed with olive fruits of the cultivar Coratina (*Olea europaea* L.) having a maturity index of 1.9; the fruits were harvested by a trunk shaker machine and processed 6 h after the harvesting. The maturity index was determined according to the method proposed by the International Olive Council [36]. Olive pomace was sampled from the decanter at regular time intervals and stored at 25 °C until analysis. The wastewater was sampled from the horizontal centrifugal separator at regular time intervals and stored at 25 °C until analysis. Three aliquots of olive oil (500 ml), obtained from each experimental test, were acquired and stored in dark bottles at 15 °C until analysis.

#### 2.3.2. Extraction yield

The extraction yield ( $EY_{EVOO}$ ) is the amount of oil obtained by milling 100 kg of olives. The EY was calculated using the following equation:

$$EY_{EVOO} = \frac{W_{oil}}{W_{olives}} \cdot 100$$

where  $W_{oil}$  is the mass of the extracted oil (kg) and  $W_{olives}$  is the mass of the processed olives (kg) [5].

#### 2.3.3. Virgin olive oils quality indices

**2.3.3.1. Legal quality parameters.** The olive oil acidity (% oleic acid per 100 g olive oil), peroxide value (meq O<sub>2</sub> kg<sup>-1</sup> oil) and UV determinations ( $K_{232}$ ,  $K_{270}$  and  $\Delta K$ ) were carried out according to the EC Reg. 2568/1991 subsequent amendments [37]. The parameters  $K_{232}$  and  $K_{270}$  are the oil absorbance at 232 and 270 nm, respectively, and  $\Delta K$  was calculated from the absorbances at 262, 268 and 274 nm. Spectrophotometric determinations,  $K_{232}$ ,  $K_{270}$  and  $\Delta K$  analyses were carried out using a Shimadzu UV-1601 spectrophotometer (Shimadzu, Kyoto, Japan). A sensory analysis was carried out by eight assessors who were fully trained in the evaluation of VOO according to the official methods of the IOC (1996) and EC Reg. 2568/1991 [37].

#### 2.3.4. Extraction of the phenolic fraction

The oil (10 g) was dissolved in 10 ml of hexane and extracted three times in a separating funnel with 7 ml of a mixture of methanol: water (60:40 v/v). The hydro-alcoholic extract was washed with hexane and centrifuged 5 min at 4000 rpm using a PK 120 centrifuge (ALC International, Milan, Italy). The methanol phase was collected and evaporated in a vacuum flask using a rotary evaporator Mod. Laborota 4000 efficient (Heidolph instruments, Milan, Italy) at 40 °C. The residue was collected using 2 ml of methanol for the HPLC injection.

#### 2.3.5. Determination of phenols

The total phenols content in the polar fraction extracted from olive oil samples was measured by colorimetric methods using Folin-Ciocalteu reagent and HPLC-UV-MSn analysis [38].

The phenolic compounds in the EVOOs were analysed as described by COI/T.20/Doc n. 29 method, with some modifications [39]. The method is based on the direct extraction of the biophenolic minor polar compounds from olive oil by means of a hydro-alcoholic solution and subsequent quantification by HPLC-DAD with the detector at 280 nm. Syringic acid is used as the internal standard. The content of the natural and oxidised oleuropein and ligstroside derivatives, lignans, flavonoids and phenolic acids is expressed in mg/kg of tyrosol (Met. COI/T.20/Doc. n. 29, 2009).

The oil (5 g) was dissolved in 10 ml of hexane, added of 1 ml of the internal standard solution (syringic acid, 0.015 mg/ml) and extracted three times in a separating funnel with 7 ml of a mixture of methanol/water (60/40 v/v). The hydro-alcoholic extract phase was collected, washed with hexane and centrifuged 5 min at 4000 rpm using a PK 120 centrifuge (ALC International, Milan, Italy). The hydro-alcoholic phase was evaporated in a vacuum flask using a rotary evaporator Mod. Laborota 4000 efficient (Heidolph instruments, Milan, Italy) at 40 °C. The residue was collected using 1 ml of methanol for the HPLC injection. HPLC analysis was performed using an HPLC Shimadzu mod. LC-10ADVP equipped with a UV-Vis (Photo) Diode Array detector (Shimadzu Italia, Milan, Italy), using a reverse phase column Spherisorb S5 ODS3 250 × 4.6 mm i.d. (Phenomenex, Castel Maggiore, BO, Italy). The following eluents phases have been used: Eluent A was water:trifluoroacetic acid (TFA) 97:3 v/v and eluent B was methanol:acetonitrile 20:80 (v/v). The elution gradient started from 5% eluent B and reached 60% B after 35 min at flow rate 1 ml/min. The injected volume was 20 µL and chromatograms were recorded at wavelength 279 nm. The acquisition software was Class-VP Chromatography data system vers. 4.6 (Shimadzu Italia, Milan, Italy). The values of the response factors (RF) for 1 µg of tyrosol and 1 µg of syringic acid were calculated, along with the ratio of the response factor of syringic acid to tyrosol, called RRF<sub>syr/tyr</sub>.

RF1µg (syringic acid) = Area syringic acid/µg syringic acid injected

RF1µg (tyrosol) = Area tyrosol/µg tyrosol injected

RRF<sub>syr/tyr</sub> = RF1µg (syringic acid)/RF1µg (tyrosol)

The value of RRF<sub>syr/tyr</sub> should be constant and should lie inside the range 5.1 ± 0.4. It allows the final result to be expressed as tyrosol, using syringic acid as the internal standard. Biophenol content (*Bio.f.c*), expressed in mg/kg, is calculated by measuring the areas of the related chromatographic peaks according to the following formula:

$$Bio.f.c = Aph * 1000 * RRF_{syr/tir} * (W_{syr.acid}) / (A_{syr.acid}) * W_{pr}$$

where:

*Aph* is peak areas of the biophenols recorded at 279 nm;

*A<sub>syr.acid</sub>* is the area of the syringic acid internal standard recorded at 279 nm;

1000 is the factor used to express the result in mg/kg;

*W<sub>pr</sub>* is the weight of the oil used, in grams;

*RRF<sub>syr/tir</sub>* is the multiplication coefficient for expressing the final results as tyrosol;

*W<sub>syr.acid</sub>* is the weight, in mg, of the syringic acid used as internal standard in 1 ml of solution added to the sample.

Phenolic compounds were identified by comparing retention times, relative elution order and UV absorbance spectra with those of authentic standards, when available, or with those reported in the literature [40–42]. Identification was confirmed by LC/MS analysis (Savarese et al., 2007).

### 2.3.6. Carotenoid content

The concentration of total carotenoids was calculated by measuring the absorption at 449 nm of 0.25 g of oil dissolved in 10 ml UV-hexane, using a calibration curve obtained previously by measuring the absorption of solutions of  $\beta$ -carotene at known concentrations.

### 2.3.7. Tocopherol compounds

Tocopherol compounds were determined by HPLC according to the method reported by Clodoveo et al. 2013 [17].

### 2.3.8. Enzyme PPO: extraction and assay

The PPO extraction procedure was the same as that reported by Clodoveo et al. 2016 [30]. Fruit samples were frozen in liquid nitrogen and pulverized with a pestle and mortar. One to five grams of frozen sample were used to obtain a dried acetone powder and stored at  $-20\text{ }^{\circ}\text{C}$ . Immediately before each PPO assay, 10 mg of acetone powder was resuspended in the proportion of 1:60 (w/v) in 0.1 M phosphate buffer, pH 6.2 with  $0.3\text{ mg ml}^{-1}$  of type-II trypsin inhibitor, stirred for 1 h at  $4\text{ }^{\circ}\text{C}$ , centrifuged at 5000g for 10 min at  $4\text{ }^{\circ}\text{C}$  and filtered through glass wool. The crude extract was used for protein quantification and PPO assays. Protein concentration was determined by the Bradford method [43]. Polyphenol oxidase activity based on an initial rate of increase in absorbance at 410 nm was determined spectrophotometrically using ultraviolet–visible spectrophotometer Ultrospec 7000 (GE, Company, UK). The assays were performed at  $30\text{ }^{\circ}\text{C}$  in a medium containing 0.1 M sodium phosphate buffer, pH 6.2, 40 mM catechol,  $10\text{ }\mu\text{l}$  of fruit enzyme extract in a total volume of 1 ml. Specific activity was expressed as  $\mu\text{mol} \times \text{min}^{-1} \times \text{mg protein}^{-1}$ .

## 2.4. Statistical analysis

Olive oil extraction experiments were performed in triplicate, and chemical analyses of the oil obtained were conducted in duplicate. The results were expressed as mean value (mv)  $\pm$  Standard Deviation (SD). Significant differences among treatments were determined using one-way ANOVA followed by “*t*-test”. Regard to the extraction and assay of enzyme PPO, the one-way analysis of

variance (ANOVA), using the Tukey's honestly significant differences (HSD) post hoc test, with the SPSS Base 11.5 software (SPSS Inc., Chicago, IL, USA) was performed. Statistical significance for the tests was set at  $p < 0.05$ .

## 3. Results

### 3.1. Fluid-dynamic results

As mentioned earlier, one of the most important evaluation criteria to study the sono-exchanger is the analysis of the pressure and velocity fields (according to Bernoulli's law) around the US probes.

Fig. 8 shows the velocity distribution along the sono-exchanger, which permits the inlet velocity ( $0.078\text{ m/s}$ ) and every critical condition to be checked, such as the flow around the head of the probes, where the value of the velocity is the maximum, namely  $0.156\text{ m/s}$ .

The flow accelerates from the inlet section because of the decreasing cross-section area and slows down when the cross-section area increases until it stops near the wall and the transducer tip (Fig. 9). The asymmetrical distribution of the velocity intensity due to the centrifugal effects is noteworthy.

Figs. 10 and 11 show the pressure contours along a section plane of the sono-exchanger and the pressure drop along the same linear pattern, respectively. Note that the pressure is highly uniform around the probes to allow an efficient energy exchange. The greatest pressure difference around the two probes, measured at the tip of each, is approx. 0.15 bar. These results confirm the validity of the chosen shape.

The overall pressure drop along the sono-exchanger due to friction (continuous losses) is 0.2414 bar, which depends both on the reduced flow area due to the transducers and to the curved pipe.

### 3.2. Quantity of energy

According to the method proposed by Clodoveo et al. in [18], many tests were conducted applying US in static conditions, varying only the operating time to perform the more suitable specific

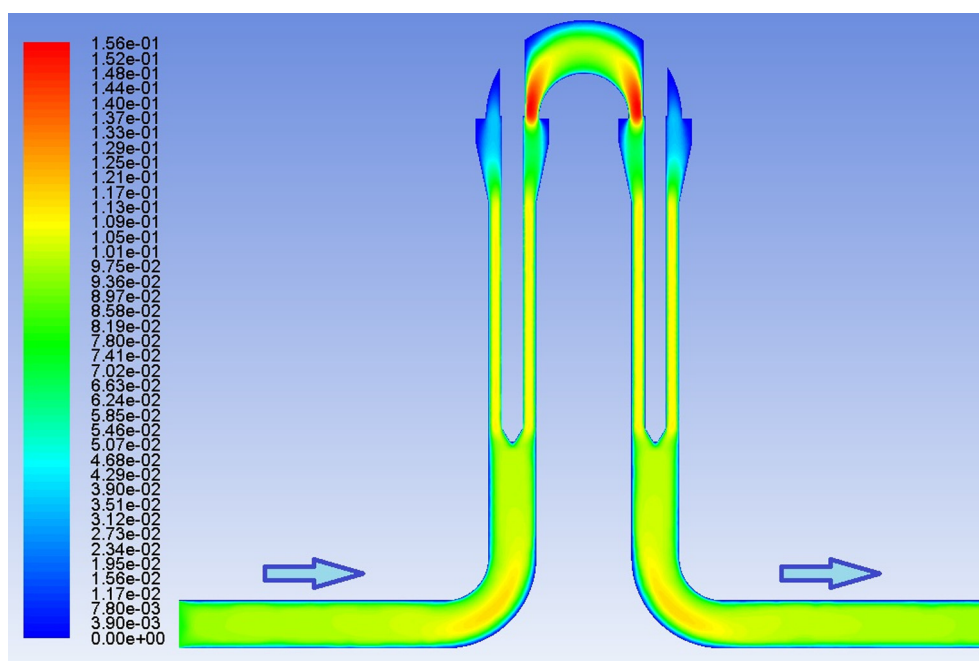


Fig. 8. Velocity contours.



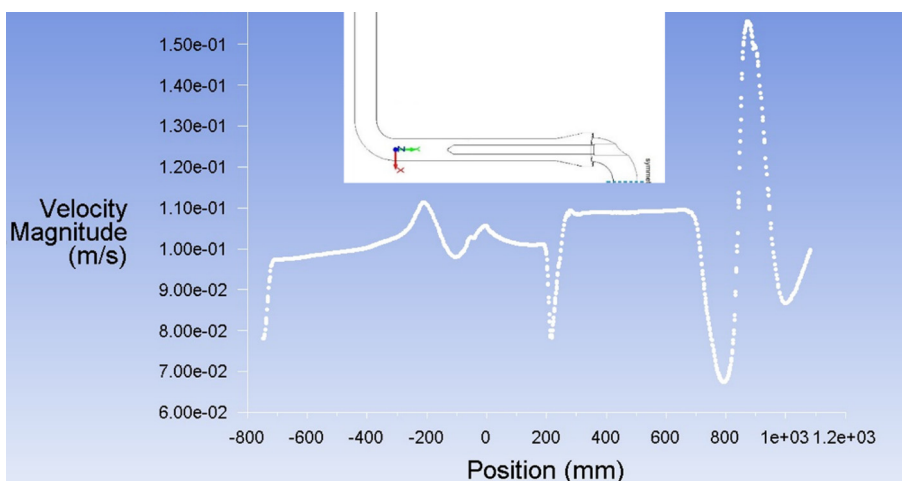


Fig. 9. Velocity trend for half geometry.

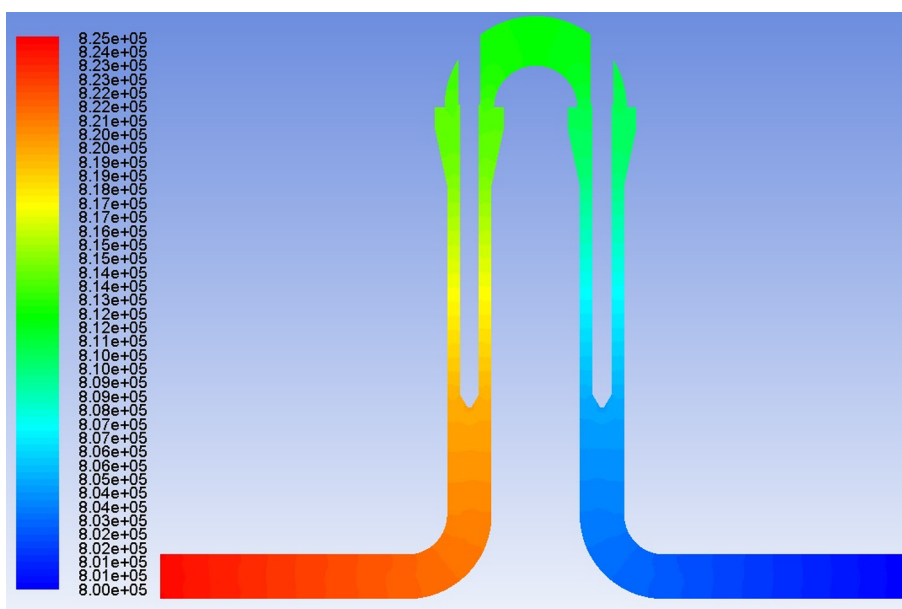


Fig. 10. Pressure contours (Pascal).

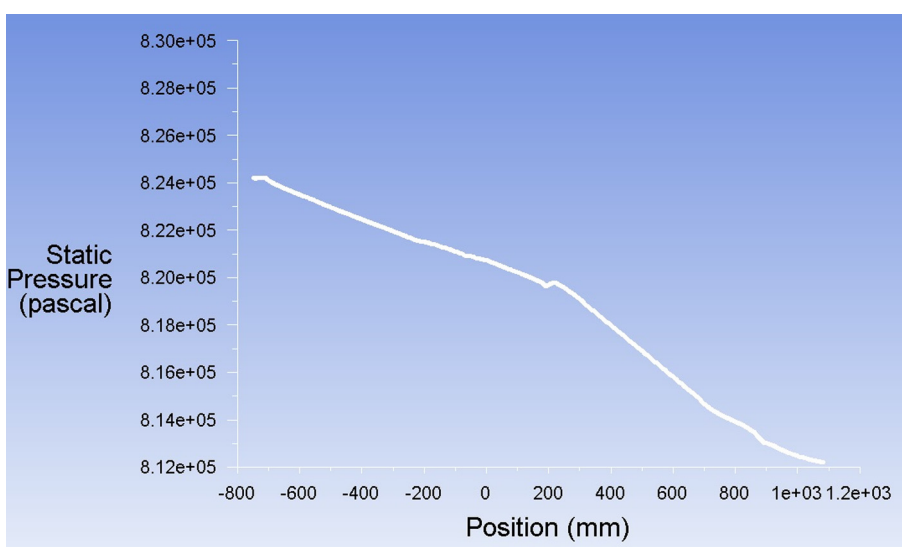


Fig. 11. Pressure drop trend along half geometry (static pressure, Pascal).

**Table 2**  
Energy provided per kg of olive paste in static conditions.

m (kg)	P <sub>s</sub> (W)	t (s)	L <sub>i</sub> (J/kg)
3	150	120	6000
3	150	180	9000
3	150	240	12000
3	150	300	15000

energy. The mass of olive paste treated was always the same, equal to 3 kg, while the transmitted power of the transducer was equal to 150 W. In Table 2 are collected the different trials where the specific energy ( $L_i$ ) is calculated applying formula (9):

These analyses demonstrate that an operating time ranging between 180 and 240 s allows obtaining the best yield and VOO quality in terms of acidity value, peroxide value and UV absorption ( $K_{270}$  and  $K_{232}$ ) [18]. In addition, the final paste temperature reached in these operating conditions is less than 27 °C, which is a threshold value to consider the extracted oil as a Virgin Olive Oil. For this duration of US treatment the specific energy transmitted to the olive paste is equal to 9000 J/kg.

In the mill plant, which comprises three US transducers, the total installed power is 4400 W; in these conditions it is necessary to have a mass flow rate equal to 0.489 kg/s (1760 kg/h) to obtain the best results. Table 3 contains the data of some extraction processes.

### 3.3. Influence of the ultrasound treatment on the extra virgin olive oil quality

#### 3.3.1. Effect on virgin olive oil quality indices

According to 2568/1991 subsequent amendments [37], EVOO is a liquid fat that conforms to a series of chemical and sensory parameters (free fatty acids < 0.8 g oleic acid/100 g oil; peroxide value < 20 meqO<sub>2</sub>/kg;  $K_{232}$  < 2.50,  $K_{270}$  < 0.22, median of defects = 0, median of fruity > 0), and is free of defects. All samples

**Table 3**  
Data recorded during the olive paste working.

	Test S1	Test S2	Test S3	Test S4	Test S5
Malaxing time (min)	30	30	–	–	–
Mass of olives (kg)	551	456	461	462	464
Crusher working time (min)	18	16	17	16	16
Crusher working time (h)	0.300	0.267	0.283	0.267	0.267
G <sub>op</sub> Mass flow rate (kg/h)	1836.67	1710.00	1627.06	1732.50	1740.00
G <sub>op</sub> Mass flow rate (kg/s)	0.5102	0.4750	0.4520	0.4813	0.4833
Inverter frequency (Hz)	20	20	18	18	18
Mass flow rate variation vs best condition	+4.36%	–2.84%	–7.55%	–1.56%	–1.14%
Power of upstream transducers (W)	3000	3000	3000	3000	3000
Power of downstream transducer (W)	1400	0	1400	1400	1400
p <sub>out</sub> Exit pressure of the sono exchanger (bar)	8.1	8.0	7.8	8.2	7.9
L <sub>i</sub> Operating specific energy (J/kg)	6468.2	4736.8	7301.5	6857.1	6827.6

**Table 4**  
Effect of ultrasound treatment on the phenolic composition (mg/kg) in olive oils cv. Coratina.

Sample	OHTy	Ty	OHTy-EDA	Ty-EDA	AP	OHTy-EA	Ty-EA	TPC	Total Carotenoids	α-Tocopherol
C <sub>1</sub>	1.5 ± 0.2a	2.9 ± 0.0a	322.5 ± 16.1b	107.4 ± 4.0a	39.9 ± 1.5a	111.6 ± 4.5a	12.0 ± 0.3a	611.2 ± 18.3a	26.88 ± 1.05a	144 ± 4.8a
C <sub>2</sub>	1.2 ± 0.3a	3.1 ± 0.2b	280.0 ± 13.4a	105.2 ± 4.2a	39.9 ± 1.4a	131.4 ± 5.4b	11.8 ± 0.2a	585.1 ± 16.8a	28.84 ± 1.12a	154.5 ± 5.15a
C <sub>3</sub>	1.8 ± 0.1ab	2.8 ± 0.1a	306.2 ± 18.4ab	107.2 ± 5.9a	41.1 ± 1.9a	112.8 ± 4.6a	13.2 ± 0.3b	598.2 ± 16.6a	27.72 ± 1.08a	148.5 ± 4.95a
S <sub>1</sub>	1.8 ± 0.1ab	3.4 ± 0.1b	387.3 ± 16.5c	115.5 ± 4.4a	41.4 ± 1.6a	112.8 ± 3.7a	12.8 ± 0.2b	684.0 ± 15.4b	36.32 ± 1.02b	241.0 ± 4.7d
S <sub>2</sub>	1.9 ± 0.1b	3.7 ± 0.1c	384.5 ± 26.8c	121.8 ± 5.8b	44.6 ± 2.0ab	143.2 ± 4.5c	13.2 ± 0.2b	728.0 ± 19.2b	35.35 ± 1.10b	242.4 ± 5.05d
S <sub>3</sub>	2.0 ± 0.1b	3.7 ± 0.2c	401.7 ± 19.0c	123.6 ± 5.6b	44.5 ± 2.4ab	161.4 ± 4.8d	15.3 ± 0.4c	768.0 ± 18.6b	33.6 ± 1.05b	230.4 ± 4.8c
S <sub>4</sub>	1.8 ± 0.1ab	3.6 ± 0.1c	389.0 ± 14.7c	134.0 ± 5.1c	47.3 ± 1.4b	134.3 ± 4.8bc	13.5 ± 0.4b	739.0 ± 18.6b	34.3 ± 1.07b	235.2 ± 4.9 cd
S <sub>5</sub>	1.6 ± 0.1a	3.1 ± 0.1a	366.0 ± 17.1c	117.7 ± 3.6b	43.9 ± 1.6ab	124.1 ± 3.2b	13.2 ± 0.4b	683.8 ± 14.2b	31.85 ± 0.99b	218.4 ± 4.55b

OHTy: hydroxytyrosol, Ty: tyrosol; Ty-EDA, dialdehydic form of elenoic acid linked to tyrosol; OHTy-EDA, dialdehydic form of elenoic acid linked to hydroxytyrosol; Ty-EA, aldehydic form of elenoic acid linked to tyrosol; OHTy-EA, aldehydic form of elenoic acid linked to hydroxytyrosol; AP: 1-acetoxy-pinoresinol; TPC: total phenol content compounds. Values are averages of three replicates (n = 3). Values followed by different letters in columns are statistically different (p < 0.05).

showed very low values of acidity, peroxide value,  $K_{232}$  and  $K_{270}$  so that they were defined as belonging to the commercial class of “extra virgin” olive oils. Considering these chemical parameters, no significant differences were found attributable to the ultrasonic treatment (p < 0.05) (data not shown). This result is in agreement with previous data available in literature [17,18].

#### 3.3.2. Influence of the ultrasound treatment on the concentration of minor compounds of EVOO

The phenolic compounds are important minor compounds in the evaluation of the quality of the EVOO. They are strongly related to the EVOO shelf life because of their antioxidant ability, have bioactive activities and are also responsible of pungent and bitter sensory attributes [19]. Furthermore they have been included in a specific health claim for virgin olive oil by European Union [18]. Total phenols showed significant higher values in the EVOO obtained applying the ultrasound treatment. These results are in contrast with previous researches. At pilot scale, Clodoveo et al. [18] observed a reduction of total phenol content of EVOO when the ultrasound treatment was applied to the crushed olive paste. These observation was confirmed in 2015 by Bejaoui et al. [16]. Clodoveo et al. [18] explained this reduction of VOO phenolics by the enhancement of the oxygen action for the non-enzymatic oxidation and its influence on the endogenous enzymes such as “Polyphenol oxidase,” “Peroxidase,” and “b-glucosidase,” as well as the orientation of the phenolics, with hydrophilic properties, to the air-oil interface. Observing Fig. 8, it is clear that the discontinuity in the olive paste delivered from the pump should be avoided. In fact, when the olive paste is not homogenous, air spaces are dispersed into the mass, favouring the oxidative reactions. The extraction tests were conducted monitoring the homogeneity of the olive paste and continuously adjusting the mass flow processed by the crusher, varying the rotational speed, because a low value causes air infiltration. In addition to the total phenol content, the composition of the phenolic fraction was determined (Table 4).

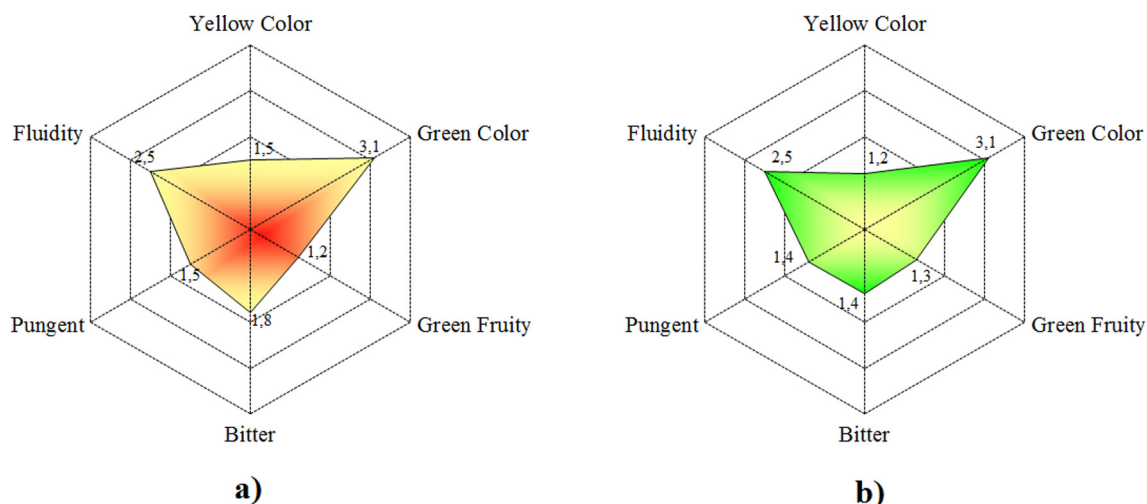


Fig. 12. Sensory evaluation of EVOO obtained by the traditional (a) and the innovative (b) ultrasound treatment of olive paste.

A significant increment of tyrosol, secoiridoid derivatives (dialdehydic form of elenolic acid linked to hydroxytyrosol (3,4-DHPEA-EDA), dialdehydic form of elenolic acid linked to tyrosol (r-HPEA-EDA), aldehydic form of elenolic acid linked to hydroxytyrosol (3,4-DHPEA-EA) I was observed for EVOO extracted after the ultrasound treatment of olive paste. The higher increase was observed for the secoiridoids derivatives p-HPEA-EDA, (17%) and 3,4-DHPEA-EA (20%). The same average was revealed for all the others compounds. In fact also the Hydroxytyrosol (3,4-DHPEA) and Tyrosol (p-HPEA) showed an increase of 14 and 15% respectively, going from control to sonicated samples (1,5 mg/kg vs 1,8 mg/kg). The lignans (+) acetoxyderivative showed an increase ranging equal to 16%. Finally a less significant value was observed for the p-HPEA-EA (11%).

With regard to the sensorial evaluation, the oils obtained by treating the olive paste with ultrasounds were characterized by a more harmonic taste than those obtained with the traditional method, with the latter being perceived more aggressive (Fig. 12). For this experimental plan the evaluation of colour is

shown in the same Fig. 12 in order to ascertain the quantity of pigments obtained by means of ultrasound.

The significant increment in polyphenols in the sonicated oils can be also attributed to the effect of ultrasound on polyphenoloxidase (PPO) activity. Fig. 13 shows the ultrasound inhibition effect of olive PPO. The EVOO quality is intimately affected by its content in phenolic compounds. PPO is responsible for oxidative losses of phenolics during olive paste malaxation. EVOO phenols play a key role in the shelf life of the product due to their activity delaying oxidation processes. They act as chain breakers by donating radical hydrogen to alkylperoxy radicals, produced by lipid oxidation and contribute to the formation of stable derivatives. Comparing the EVOOs samples extracted by means the traditional and the innovative system, an average increase of about 48% of  $\alpha$ -tocopherols and of about 30% of carotenoids were observed after ultrasound treatment.

#### 4. Conclusion

The application of ultrasounds to the virgin olive oil production process can offer an interesting number of advantages due to their mechanical and thermal effects. The ultrasound technology is able to induce the rupture of cell walls, recovering the oil and minor compounds trapped in the uncrushed olive tissue, thus increasing the work capacity of the extraction plant and reducing the process time. One of the most important challenge of this paper is to design, by means of a thorough CFD analysis, and to build a sono-exchanger able to improve the working capacity of the industrial plants, performing an effective continuous process. The fluid dynamic analysis was performed by means of a commercial software package to predict the flow path around the ultrasound devices and to evaluate the flow parameters of the olive paste inside the sono-exchanger. The influence of each geometrical parameter was assessed to setup an optimal design of the sono-exchanger, and the results demonstrate that the pressure drops and velocity fields are suitable to ensure the best ultrasounds diffusion. The experimental campaign, performed on a real scale mill plant, demonstrates that no alteration in the EVOO quality parameters were observed after the ultrasound treatment. The ultrasound treatment gave oils with significantly higher contents of tocopherols, carotenoids, and phenolics. The significant polyphenols increment in the sonicated oils can be also attributed to the effect of the ultrasounds on the polyphenoloxidase activity. More-

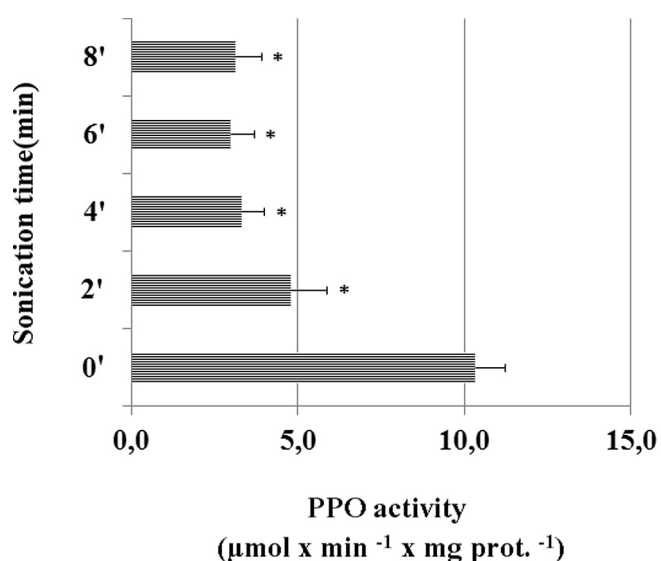


Fig. 13. Ultrasound inhibition effect of olive PPO. Olive paste was sonicated for 2, 4, 6, and 8 min before malaxation. Asterix indicate statistical significance vs control untreated (Anova test,  $p < 0.05$ ).

over, the ultrasounds improved the sensory evaluation of the samples.

### Acknowledgements

The engineering design and the prototype development were realized with the financial support of EU through the Regione Molise: Fondo europeo agricolo per lo sviluppo rurale: l'Europa investe nelle zone rurali ai sensi della Misura 124 (seconda edizione) del PSR Molise 2007/2013. Determinazione di concessione n. 108 del 18/02/2014.

The EVOO quality evaluation was realized with the financial support of EU through the Regione Puglia: Programma Regionale a Sostegno della Specializzazione Intelligente e della Sostenibilità Sociale ed Ambientale – Intervento “FUTURE IN RESEARCH” Università: Università degli Studi di Bari “A. Moro” Dipartimento: Dipartimento di Scienze Agro Ambientali e Territoriali (DISAAT) – Titolo Del Progetto – Ultrasuoni nel processo di estrazione dell'olio vergine di oliva and the financial support of EU through the Regione Puglia: “Avviso Aiuti a Sostegno dei Cluster Tecnologici Regionali per l'Innovazione” – Progetto: “PERFORM TECH (PUGLIA EMERGING FOOD TECHNOLOGY) – La sicurezza alimentare mediante l'impiego di tecnologie emergenti per l'elaborazione di prodotti funzionali, recupero di sostanze nutraceutiche dai sottoprodotti e valorizzazione energetica degli scarti” – codice LPIJ9P2.

The evaluation of ultrasound as a tool useful to increase the nutraceutical and economic value of the product has been supported by the AGER Foundation by means of the project Claims of Olive oil to iMProVE The market ValuE of the product. – COMPETITIVE.

The authors are grateful to the Official Tasting Panel of Virgin Olive Oils of Molise Region for the sensory evaluation of samples. The authors also thank Filomena Aloia and Giovanni Aloia (Managers of Aloia farm), as well as Michele Mizzi and Vito Mele for their support in the experimental campaign.

### References

- [1] R. Amirante, M.L. Clodoveo, E. Distaso, F. Ruggiero, P. Tamburrano, A tri-generation plant fueled with olive tree pruning residues in Apulia: An energetic and economic analysis, *Renewable Energy* 89 (2016) 411–421.
- [2] M.L. Clodoveo, S. Camposeo, B. De Gennaro, S. Pascuzzi, L. Roselli, In the ancient world, virgin olive oil was called “liquid gold” by Homer and “the great healer” by Hippocrates. Why has this mythic image been forgotten?, *Food Res Int.* 62 (2014) 1062–1068.
- [3] M.L. Clodoveo, T. Dipalmo, P. Crupi, V. Durante, V. Pesce, A. Lovece, A. Mercurio, A. Laghezza, F. Corbo, C. Franchini, Comparison between different flavored olive oil production techniques: healthy value and process efficiency, *Plant Foods Hum. Nutr.* (2016) 1–7.
- [4] M.L. Clodoveo, S. Camposeo, R. Amirante, G. Dugo, N. Cicero, D. Boskou, Research and Innovative Approaches to Obtain Virgin Olive Oils with a Higher Level of Bioactive Constituents in the book: *Olives and Olive Oil Bioactive Constituents*, in: D. Boskou (Ed.), AOCS Press, Urbana, IL – USA, 2015, ISBN: 978-1-630670-41-2, pp 179–216.
- [5] M.L. Clodoveo, Malaxation: Influence on virgin olive oil quality. Past, present and future—An overview, *Trends Food Sci. Technol.* 25 (1) (2012) 13–23.
- [6] M.L. Clodoveo, New advances in the development of innovative virgin olive oil extraction plants: Looking back to see the future, *Food Res. Int.* 54 (1) (2013) 726–729.
- [7] M.L. Clodoveo, R.H. Hbaieb, F. Kotti, G.S. Mugnozza, M. Gargouri, Mechanical strategies to increase nutritional and sensory quality of virgin olive oil by modulating the endogenous enzyme activities, *Compreh. Rev. Food Sci. Food Safety* 13 (2) (2014) 135–154.
- [8] M.L. Clodoveo, T. Dipalmo, C. Schiano, D. La Notte, S. Pati, What's now, what's new and what's next in virgin olive oil elaboration systems? A perspective on current knowledge and future trends, *J. Agric. Eng.* 45 (2) (2014) 49–59.
- [9] M.L. Clodoveo, An overview of emerging techniques in virgin olive oil extraction process: Strategies in the development of innovative plants, in: *Proceedings of AIAA Conference, Viterbo, Italy, 8–12 September 2013* *Journal of Agricultural engineering*, XLIV, Supplement 1, 2013, 297–305.
- [10] F. Chemat, M.K. Khan, Applications of ultrasound in food technology: processing, preservation and extraction, *Ultrason. Sonochem.* 18 (4) (2011) 813–835.
- [11] J. Chandrapala, C. Oliver, S. Kentish, M. Ashokkumar, Ultrasonics in food processing, *Ultrason. Sonochem.* 19 (5) (2012) 975–983.
- [12] M. Ashokkumar, Applications of ultrasound in food and bioprocessing, *Ultrason. Sonochem.* 25 (2015) 17–23.
- [13] A. Patist, D. Bates, Ultrasonic innovations in the food industry: from the laboratory to commercial production, *Innov. Food Sci. Emerg.* 9 (2008) 147–154.
- [14] A. Jiménez, G. Beltrán, M. Uceda, High-power ultrasound in olive paste pretreatment. Effect on process yield and virgin olive oil characteristics, *Ultrason. Sonochem.* 14 (2007) 725–731.
- [15] G. Cravotto, L. Boffa, S. Mantegna, P. Perego, M. Avogadro, P. Cintas, Improved extraction of vegetable oils under high-intensity ultrasound and/or microwaves, *Ultrason. Sonochem.* 15 (5) (2008) 898–902.
- [16] M.A. Bejaoui, G. Beltran, A. Sánchez-Ortiz, S. Sanchez, A. Jimenez, Continuous high power ultrasound treatment before malaxation, a laboratory scale approach: Effect on virgin olive oil quality criteria and yield, *Eur. J. Lipid Sci. Technol.* (2015).
- [17] M.L. Clodoveo, V. Durante, D. La Notte, R. Punzi, G. Gambacorta, Ultrasound-assisted extraction of virgin olive oil to improve the process efficiency, *Eur. J. Lipid Sci. Technol.* 115 (9) (2013) 1062–1069.
- [18] M.L. Clodoveo, V. Durante, D. La Notte, Working towards the development of innovative ultrasound equipment for the extraction of virgin olive oil, *Ultrason. Sonochem.* 20 (5) (2013) 1261–1270.
- [19] M.L. Clodoveo, R.H. Hbaieb, Beyond the traditional virgin olive oil extraction systems: Searching innovative and sustainable plant engineering solutions, *Food Res. Int.* 54 (2) (2013) 1926–1933.
- [20] R. Amirante, M.L. Clodoveo, Developments in the design and construction of continuous full-scale ultrasonic devices for the EVOO industry, *Eur. J. Lipid Sci. Technol.* (2016), <http://dx.doi.org/10.1002/ejlt.201600438>.
- [21] R.A. Roy, Cavitation sonophysics, *Sonochemistry and Sonoluminescence*, Springer, Netherlands, 1999, pp. 25–38.
- [22] P.M. Seya, C. Desjouis, J.C. Bera, C. Insera, Hysteresis of inertial cavitation activity induced by fluctuating bubble size distribution, *Ultrason. Sonochem.* 27 (2015) 262–267.
- [23] C. Desjouis, M. Fouqueray, C.W. Lo, P.M. Seya, J.L. Lee, J.C. Bera, C. Insera, Counterbalancing the use of ultrasound contrast agents by a cavitation-regulated system, *Ultrason. Sonochem.* 26 (2015) 163–168.
- [24] R. Amirante, E. Distaso, P. Tamburrano, Experimental and numerical analysis of cavitation in hydraulic proportional directional valves, *Energy Convers. Manage.* 87 (2014) 208–219.
- [25] H.M. Santos, C. Lodeiro, J.L. Capelo-Martínez, The power of ultrasound, vol. 171. Wileyvch Verlag GmbH & Co. KGaA, Weinheim, 2009.
- [26] P. Amirante, M.L. Clodoveo, G. Dugo, A. Leone, A. Tamborrino, Advance technology in virgin olive oil production from traditional and de-stoned pastes: influence of the introduction of a heat exchanger on oil quality, *Food Chem.* 98 (2005) 797–805.
- [27] M. Legay, B. Simony, P. Boldo, N. Gondrexon, S. Le Person, A. Bontemps, Improvement of heat transfer by means of ultrasound: Application to a double tube heat exchanger, *Ultrason. Sonochem.* 19 (6) (2012) 1194–1200.
- [28] R. Amirante, L.A. Catalano, P. Tamburrano, The importance of a full 3D fluid dynamic analysis to evaluate the flow forces in a hydraulic directional proportional valve, *Eng. Computat.* 31 (5) (2014) 898–922.
- [29] R. Amirante, L.A. Catalano, C. Poloni, P. Tamburrano, Fluid-dynamic design optimization of hydraulic proportional directional valves, *Eng. Optimizat.* 46 (10) (2014) 1295–1314.
- [30] M.L. Clodoveo, T. Dipalmo, P. Crupi, V. Durante, V. Pesce, I. Maiellaro, C. Franchini, Comparison between different flavored olive oil production techniques: healthy value and process efficiency, *Plant Foods Hum. Nutr.* 71 (1) (2016) 81–87.
- [31] R. Amirante, P. Catalano, PH—postharvest technology: fluid dynamic analysis of the solid–liquid separation process by centrifugation, *J. Agric. Eng. Res.* 77 (2) (2000) 193–201.
- [32] M. Legay, S. Le Person, N. Gondrexon, P. Boldo, A. Bontemps, Performances of two heat exchangers assisted by ultrasound, *Appl. Therm. Eng.* 37 (2012) 60–66.
- [33] R. Amirante, A. Paduano, Ultrasound in Olive Oil Extraction, in the book: “Products from Olive Tree”, edited by Dimitrios Boskou and Maria Lisa Clodoveo, ISBN 978-953-51-2725-3, Print ISBN 978-953-51-2724-6, Intech open science, 2016.
- [34] P. Amirante, A. Tamborrino, A. Leone, M.L. Clodoveo, Assessment of the viscosity value in olive oil paste using different blade rotation speed in an innovative mixer, in: *Central theme, technology for all: sharing the knowledge for development. Proceedings of the International Conference of Agricultural Engineering, XXXVII Brazilian Congress of Agricultural Engineering, International Livestock Environment Symposium–ILES VIII, Iguassu Falls City, Brazil, 31st August to 4th September, 2008. International Commission of Agricultural Engineering (CIGR), Institut fur Landtechnik, 2008.*
- [35] G.C. Di Renzo, G. Colelli, Flow behavior of olive paste, *Appl. Eng. Agric.* 13 (6) (1997) 751–755.
- [36] IOOC, 2001. Trade Standard Applying to Olive Oil and Olive Pomace Oil. International Olive Oil Council, in: *COI/T.15/NC no. 2/Rev. 10; COI/T.20/Doc. no. 24.*
- [37] European Commission Regulation No 61/2011 of 24 January 2011 amending Regulation (EEC) No 2568/91 on the characteristics of olive oil and olive-residue oil and on the relevant methods of analysis. *Official J. Eur. Union L 23/1, 27.1.2011.*

- [38] S. Alessandri, F. Ieri, A. Romani, Minor polar compounds in extra virgin olive oil: correlation between HPLC-DAD-MS and the folin-Ciocalteu spectrophotometric method, *J. Agric. Food Chem.* 62 (4) (2014) 826–835.
- [39] R. Sacchi, A. Paduano, F. Fiore, D. Della Medaglia, M.L. Ambrosino, I. Medina, Partition behavior of virgin olive oil phenolic compounds in oil-brine mixtures during thermal processing for fish canning, *J. Agric. Food Chem.* 50 (10) (2002) 2830–2835.
- [40] G.F. Montedoro, M. Servilli, M. Baldioli, R. Selvagini, E. Miniati, A. Macchioni, Simple and hydrolyzabile compounds in virgin olive oil. 3. Spectroscopic characterizations of secoridoid derivatives, *J. Agric. Food Chem.* 41 (1993) 2228–2234.
- [41] R. Mateos, J.L. Espartero, M. Trujillo, J.J. Rios, M. León-Camacho, F. Alcudia, A. Cert, Determination of phenols, flavones, and lignans in virgin olive oils by Solid-Phase Extraction and High-Performance Liquid Chromatography with Diode Array Ultraviolet Detection, *J. Agric. Food Chem.* 49 (2001) 2185–2192.
- [42] M. Brenes, J.H. Hidalgo, A. Garcia, J.J. Rios, P. Garcia, R. Zamora, A. Garrido, Pinoresinol and 1-acetoxypinoresinol, two new phenolic compounds identified in olive oil, *J. Am. Oil Chem. Soc.* 77 (2000) 715–720.
- [43] M.M. Bradford, A rapid and sensitive method for the quantitation of microgram quantities of protein utilizing the principle of protein-dye binding, *Anal. Biochem.* 72 (1–2) (1976) 248–254.